CHEMICAL ENGINEERING TRANSACTIONS
VOL. 84, 2021
A publication of AIDIC
The Italian Association of Chemical Engineering
Online at www.cetjournal.it
Guest Editors: Paolo Ciambelli, Luca Di Palma

ISBN 978-88-95608-82-2; **ISSN** 2283-9216

DME Production via Methanol Dehydration with H form and Desilicated ZSM-5 Type Zeolitic Catalysts: Study on the Correlation Between Acid Sites and Conversion

Francesco Dalena, Emanuele Giglio, Gianfranco Giorgianni, Daniela Cozza, Alessia Marino, Alfredo Aloise
Laboratory of Industrial Chemistry and Catalysis, University of Calabria, Via Pietro Bucci, I-87036, Rende, CS, Italy
emanuele.giglio@unical.it

Methanol (MeOH) dehydration for Dimethyl ether (DME) production is one of the possible pathways to produce a green, synthetic fuel that can substitute fossil/conventional ones in automotive/transportation applications. DME synthesis in gas phase usually occurs in presence of an acid catalyst at moderate temperature (up to 250 °C). This work deals with the use of MFI-type zeolitic catalysts. H form and desilicated zeolite samples were synthesized, characterized, and tested to investigate their catalytic activity in MeOH dehydration reaction. Ammonia temperature-programmed desorption (NH_3-TPD) and Fourier-transform Infrared spectroscopy (FT-IR) analyses were carried out to elucidate the amount and the nature of acid sites. Zeolite sample desilicated for 60 minutes presented a higher amount of Bronsted acid sites (that can be correlated to the superior catalytic activity), while the Turnover frequency (TOF) referred to the amount of Bronsted acid sites is very similar for the investigated samples. Finally, preliminary kinetic investigation via linear fitting of experimental data on the Arrhenius plot was carried out for simple first and second order kinetic models.

1. Introduction

The rapid growth in global energy demand, greenhouse gas emissions, and global warming, associated with the use of fossil fuels, is stimulating a continuous research for alternative and renewable fuels showing a very low environmental impact (Papanikolaou et al., 2020). Research efforts have been thus made on low cost and large-scale processing for biofuels both as a renewable resource using second and third generation feedstocks (Abate et al., 2016), and with low environmental impact. Renewable energy sources can be exploited to produce green and eco-friendly fuels as hydrogen (Iulianelli et al., 2019), methane, alcohols (Dalena et al., 2019), syncrude (Marchese et al., 2020) and Dimethyl Ether (DME). DME is a non-toxic and non-corrosive organic compound that can be employed as intermediate compound in the production of olefins. Due to high cetane number and low NOx emissions during combustion, it is used as a clean substitute of diesel fuel and Liquid Petroleum Gas (LPG) (Migliori et al., 2020). DME is produced via methanol dehydration (eq 1):

$$2CH_3OH \rightleftarrows CH_3OCH_3 + H_2O \quad (1)$$

This reaction is usually carried out in presence of a solid-acid catalyst as γ-alumina and acid zeolites. MFI (ZSM-5) samples show significantly higher catalytic activity (Rownaghi et al., 2012).
The formation of DME can mainly take place through associative or dissociative pathway (Park et al., 2020). ZSM-5 superior activity than γ-alumina-type catalysts can be thus related to the considerable difference in acid sites concentration. ZSM-5 type zeolite supported membranes were also used in catalytic membrane reactors for DME synthesis (Brunetti et al., 2020). Recent studies (Aloise et al., 2020) have shown how hierarchical (or mesoporous) zeolites induced by alkaline solutions on ZSM-5 zeolites leads to a marked improvement in the performance of the catalyst in terms of deactivation for MeOH to DME reactions of the catalyst. The intrinsic microporosity of zeolitic catalysts often imposes limitations on molecular diffusion due to the hindered access

inside the crystalline structure. Mesoporous zeolites partially give a solution to these problems by adding an auxiliary network of inter and/or intra-crystalline mesopores. The induced mesoporosity increases the number of accessible micropores and effectively shortens the average length of the path to the active sites, thereby increasing the catalytic performance (Meunier et al., 2012).
In this work a correlation between acid sites of ZSM-5 and hierarchical ZSM-5 catalysts has been investigated for the dehydration reaction of methanol in the temperature range of 140-240 °C.

2. Experimental

2.1 Samples preparation

The H form zeolite catalyst was synthesized according to the procedure described in the literature (Migliori et al., 2014), by using the following synthesis gel composition: 1 SiO_2 - 0.02 Al_2O_3 - 0.08 Na_2O - 0.08 TPABr - 20 H_2O. The reaction was carried out under stirring for 2h at room temperature starting from Tetrapropylammonium Bromide (TPABr98%, Fluka) as Structure Directing Agent (SDA), sodium hydroxide (NaOH 97%, Carlo Erba Reagenti), sodium aluminate anhydrous (Sigma Aldrich), ultrapure water and silica gel precipitate (100% SiO2, Merck) as a source of silica under stirring. The mixture was transferred in a static oven and heated at 170 ° C for 4 days. After crystallization, the catalyst was firstly calcined to remove the SDA in a tubular oven at 550°C for 6 hours, then an ion exchange was performed twice with a 1M solution of NH_4Cl at 80°C for 2 hours to convert the Na-form to NH_4-form. Finally, the sample was calcined again under the same condition as the first calcination to remove the ammonium cations.
In order to obtain a hierarchical phase according to the literature procedure (Aloise et al., 2020), the H form sample (ZSM5_P) was desilicated with a NaOH solution (0.1M at 65 °C) with a ratio zeolite/solution equal to 1g/20ml at two different contact times: 30 min (ZSM5_30) and 60 min (ZSM5_60).

2.2 Physicochemical characterization

The Si/Al ratio in the zeolite was measured by atomic absorption analysis (GBC 932 AA). The effect of the desilication process was evaluated by nitrogen adsorption/desorption isotherms at -196 ° C (ASAP 2020, Micromeritics). Specific surface areas were calculated by the BET (Brunauer, Emmett and Teller) method, using the Rouquerol transform. Total pore volumes and micropore volumes were estimated by the t-plot method.
The concentration of the acid sites was estimated by temperature-programmed desorption (ammonia-TPD) and Fourier-transform infrared spectroscopy (FT-IR) analysis. NH_3-TPD (TPDRO1100, ThermoFisher) was carried out according to a previously reported procedure (Catizzone et al., 2017). The analysis consists of a first ammonia adsorption phase inside the catalyst (pretreatment) and a desorption phase programmed with a thermal ramp (10 °C/min) in the temperature range from 100 to 700 °C. FT-IR spectra were measured by using a Nicolet iS 10 – FT-IR Spectrometer (Thermoscientific, USA) with an optical resolution of 4 cm^{-1} and equipped with a DTGS detector. The samples were pressed into disks with a radius of 1.3 cm and a weight of about 25 mg. The disks were outgassed at 10^{-5} torr under heating (400 °C for 2h, heating rate of 10 °C/min). FT-IR spectra were recorded in the mid-IR (4000-400 cm^{-1}). Deuterated acetonitrile (CD_3CN) was used as weak basic probe molecule via the adsorption on the activated samples at 30 °C for 30 min to estimate the concentration of Bronsted and Lewis acid sites. D_3-acetonitrile in excess was subsequently removed by vacuum evacuation at 10^{-4} - 10^{-5} torr for 10 h. The obtained spectra were analysed by integration using specialised Thermo software, OMNIC (Thermo Scientific) and the bands were integrated by using a peak deconvolution procedure (Peak Fit Software). The D_3-acetonitrile concentration on the specific acid site (Bronsted and Lewis) was calculated as follows:

$$C\ (\mu mol\ g_{cat}^{-1}) = \frac{IA\ (X)}{\varepsilon(X) * \sigma} \quad (2)$$

Where IA(X) is the integrated absorbance of the peak of the acid species X (Lewis or Bronsted) and σ is the density of the wafer, while ε is the extinction coefficient of the D_3-acetonitrile for the acid species X.

2.3 Catalytic tests

The H form zeolite and its corresponding hierarchical phases were tested in the experimental apparatus already described in a previous work (Migliori et al., 2018). Catalytic tests were carried out at atmospheric pressure in the temperature range 140-240 °C. A gaseous reacting mixture with controlled methanol molar fraction (≈ 6 %) and nitrogen was fed to a quartz tubular reactor loaded with 140 mg of catalyst (particle size in the range 300-500 μm). Outlet gas composition was analyzed using an inline gas chromatograph (GC-MS, Agilent 7820A) equipped with a DB1 column (Agilent J&W 125-1032, length 30 m, φ = 0.53 mm, film thickness

1.50 μm) and Ionization Detector (FID). Turnover Frequency (TOF) was calculated to measure the catalyst activity referred to the overall amount of Bronsted acid sites:

$$\mathrm{TOF}\ (mol_{MeOH} \cdot mol_{BAS}^{-1} \cdot h^{-1}) = \frac{\frac{WHSV}{\mathrm{MW}_{MeOH}} \cdot X_{MeOH}}{\mathrm{Br\ddot{o}nsted\ acid\ sites}} \quad (3)$$

Where $WHSV$ and MW_{MeOH} are weighted hourly space velocity (expressed in $g_{MeOH}\ g_{cat}^{-1}\ h^{-1}$) and methanol molecular weight, respectively. X_{MeOH} represents the experimentally evaluated methanol conversion. Conversion results can be used to estimate the kinetic parameters for methanol dehydration reaction (Catizzone et al., 2021). If first order reaction is considered, integration of kinetic equation leads to the following expression for the rate constant (Catizzone et al., 2020):

$$k = k_0 \cdot exp\left(-\frac{E_a}{R \cdot T}\right) = -\frac{\dot{n}_{R,in}}{C_{MeOH,in} \cdot m_{cat}} \cdot \ln(1 - X_{MeOH}) \quad (4)$$

Where k_0, E_a, R, $\dot{n}_{R,in}$, $C_{MeOH,in}$, and m_{cat} are pre-exponential factor, activation energy, gas constant, reactant inlet mole flow, reactant concentration and catalyst load, respectively. If second order reaction is considered, integration results in a different form for the constant rate calculation:

$$k = k_0 \cdot exp\left(-\frac{E_a}{R \cdot T}\right) = \frac{\dot{n}_{R,in}}{C_{MeOH,in}^2 \cdot m_{cat}} \cdot \frac{X_{MeOH}}{(1 - X_{MeOH})} \quad (5)$$

Once k is calculated, activation energy (E_a) and pre-exponential factor (k_0) can be estimated through a linear fitting of experimental results on the Arrhenius plot (ln[k] vs. 1/T).

3. Results and discussion

3.1 Porosity and acidity assessment

The composition, textural and acidic properties of the prepared samples were reported in Table 1. After desilicating the ZSM-5 sample for 30 and 60 min, in agreement with the selective removal of Si from the framework, the molar Si/Al ratio, as observed by AAS, decreased by 25 and an 37% (Table 1). Moreover, with respect to the parent ZSM-5, after desilicating for 30 min, the BET surface area and mesopore volume increased by 9 and 107% (Table 1), at the expense of the microporous surface area and volume, decreasing by 35% and 10%, respectively. Conversely, after the 60 min desilication treatment, the BET surface area was similar to the ZSM-5 sample, while the micropore volume and surface area decreased even with respect to the ZSM-5_30 sample.

NH_3-TPD enables the classification of catalysts acid sites into two classes: weak and strong acid sites. The former ones are related to a peak for the desorption of ammonia at a lower temperature of ≈ 270 °C, while the latter ones (strong sites) present maximum ammonia desorption at a temperature of about 450 °C. FT-IR spectra (with particular attention to the 3750 - 3550 cm^{-1} region) of the catalysts after degassing (Figure 1A) shows different bands that represent different stretching of the OH groups and their attribution is given by literature data. Investigated samples clearly show different profiles and the main differences are found between the H form sample and the two desilicated catalysts. All samples show a wider band in the 3600-3620 cm^{-1} region attributed to the square-bridged hydroxyl groups (AlOHSi) corresponding to the Bronsted sites. The first difference is in the region of the OH stretching assigned to the extra-framework AlOH groups (3670-3630 cm^{-1}): in the H form sample, the adsorption in this range is very low, while in the two desilicated samples the adsorption is more evident. The second difference lies in the adsorption zone of the weakly perturbed SiOH silanol groups (3750–3700 cm^{-1}) present in the disilicate samples, but negligible in the H form one. This difference appears evident after the adsorption of the D_3-acetonitrile probe. The basic strength of the probe does not allow the formation of hydrogen bonds between the most of the silanol groups and the weak base. For this reason, while the peaks related to the OH stretching of the stronger acid groups (3670-3620 cm^{-1}) tend to disappear after the adsorption of D_3-acetonitrile, those referring to the silanol groups are not sufficiently acidic to form hydrogen bond-type interactions with the probe and they are thus characterized by unchanged area after adsorption (Trombetta et al., 2000). According to literature data (Daniell et al., 2001; Areán et al., 2000), the adsorption bands of ν (C≡N) groups of the D_3-acetonitrile stretching vibration at 2325, 2300, 2278, and 2265 cm^{-1} are attributed to the adsorption on Lewis alumina sites, bridging OH groups, terminal SiOH groups and physisorbed liquid CD_3CN, respectively. The interaction with Bronsted sites is responsible for the 2297-cm^{-1} adsorption and is due to formation of hydrogen bond of the type O-H□□□N-CD_3 between sites and the D_3-acetonitrile (Figure 1B). Concentration results from the FT-IR spectra due to adsorbed D_3-acetonitrile are shown in Table 1.

The results concerning the total acidity of the system are comparable between the two techniques used. Desilication treatment has brought about a change in the nature of the acid sites. At shorter desilication times (30 min), the concentration of Bronsted acid sites does not change, while an increase in Lewis acid sites is observed, associable with the adsorption difference already noted previously in the 3620 cm^{-1} area (Figure 1A) and associated with the extra framework AlOH area. Different results are obtained for prolonged desilication times. For ZSM5_60 catalyst, there is an increase both in Lewis (but still lower than in the ZSM5_30 sample) and Bronsted acid sites (with a net increase of 106 $\mu mol/g_{cat}$). This increase in terms of acidity of the catalysts with induced mesoporosity may be due to the high aluminium content present in the zeolite structure. Al stabilizes silicon atoms, partially limiting the formation of mesopores. Therefore, only relatively small fractions of silicon tend to dissolve, leading to an increase in structural defects proportional to an increase in the concentration of Bronsted acid sites.

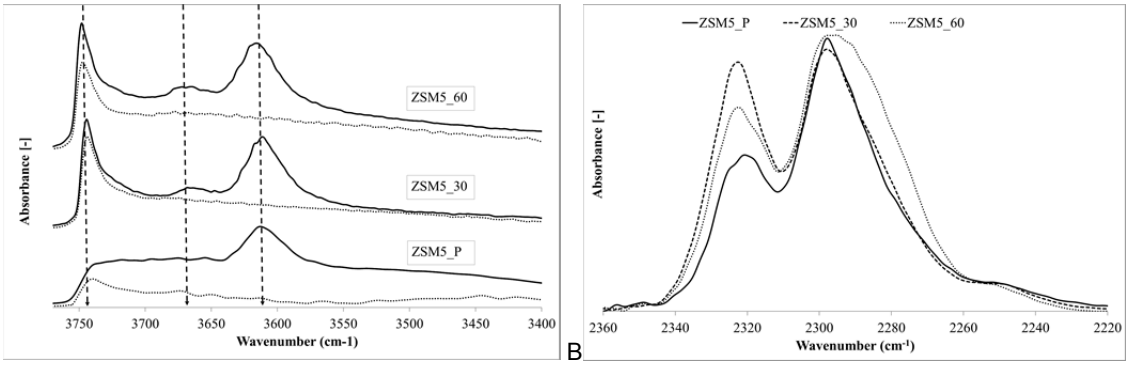

Figure 1. FT-IR spectra of the ZSM5_P, ZSM5_30, ZSM5_60 catalysts. A) spectra of the 3750 - 3400 cm^{-1} region of the activated sample (solid line) and of the samples after probe adsorption (dashed line). B. Differences between the three catalysts in terms of adsorbed acetonitrile (2360-2220 cm^{-1})

Table 1: Catalysts acidity via NH_3-TPD and FT-IR analysis

Sample	AAS	Porosimetry				NH_3TPD		FT-IR			
	Si/Al Bulk[a]	S_{BET}[b]	S_{mic}[c]	V_{mic}[c]	V_{mes}[d]	Weak AS[e]	Strong AS[f]	Brönsted AS[g]	Lewis AS[g]	Total AS[g]	B/L ratio
	(mol/mol)	(m^2/g)		(cm^3/g)		(μmol_{NH3}/gcat)		(μmol/gcat)			(-)
ZSM5_P	*35.66*	*410*	*289*	*0.17*	*0.089*	*104*	*379*	*404*	*85*	*489*	*4.73*
ZSM5_30	*26.83*	*447*	*261*	*0.11*	*0.184*	*123*	*463*	*403*	*200*	*603*	*2.01*
ZSM5_60	*22.5*	*406*	*243*	*0,10*	*0.185*	*136*	*539*	*510*	*179*	*689*	*2.83*

[a] Determined by atomic absorption analysis
[b] BET specific surface areas
[c] Micropore volumes calculated by the t-plot method
[d] Mesoporous volume, calculated by the difference between total pore volumes and micropore volumes
[e] Calculated by NH_3TPD in the range 150°C-325°C
[f] Calculated by NH_3TPD > 325°C
[g] Determined by FT-IR after adsorption of D_3-acetonitrile

3.2 Catalytic activity and kinetics

Methanol to DME reaction was investigated to assess the catalytic activity of H form and desilicated samples. Figure 2 shows the MeOH conversion pattern in the temperature range 140-240 °C. For all the investigated samples conversion increases with temperature until it approaches chemical equilibrium value at about 240 °C. Conversion difference between the tested samples is thus more evident at lower temperatures, where the H form sample and the desilicated one at 30 min present similar conversion values despite having very different total acidity values, while the desilicated sample at 60 min shows superior conversion. Therefore, catalytic activity seems to be proportional to the Bronsted acid sites concentration.

This trend is confirmed by the calculation of turnover frequency (TOF) far from equilibrium (at 160 and 180 °C). TOF provides information related to the reaction rate referred to the concentration of Bronsted acid sites

(Table 2). The results show that, although both the conversion and the concentration of the Bronsted acid sites are different, calculated TOF is similar for all the investigated samples.

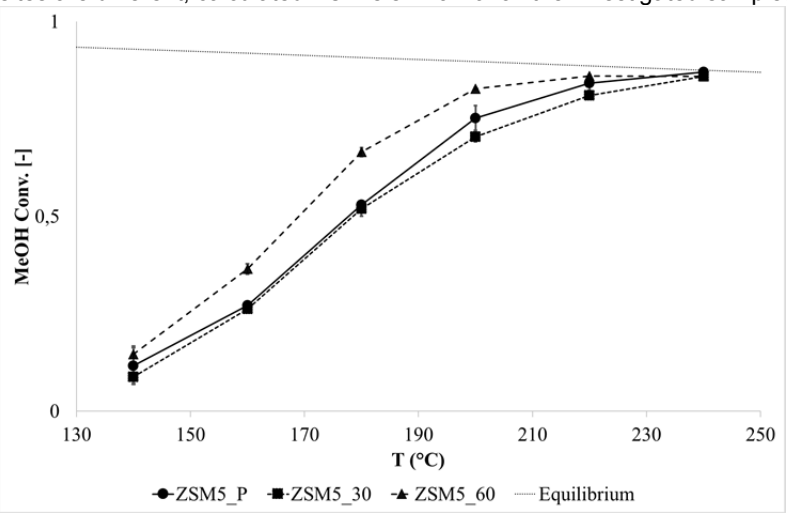

Figure 2. MeOH converted as a function of the reaction temperature for ZSM5_P (●), ZSM5_30 (■) and ZSM5_60 (▲). Test conditions— MeOH: 5.6 mol%; carrier flow rate: 60 NmL/min; WHSV: 2 $g_{MetOH}/(g_{cat}\ h)$.

Table 2: Methanol conversion and TOF data at 160 °C and at 180 °C

	160°C		180°C	
Sample	MeOH Conversion (-)	TOF ($mol_{MeOH}\ mol_{BAS}^{-1}\ h^{-1}$)	MeOH Conversion (-)	TOF ($mol_{MeOH}\ mol_{BAS}^{-1}\ h^{-1}$)
ZSM5_P	0.27	49.7	0.53	96.4
ZSM5_30	0.26	48.4	0.52	98.1
ZSM5_60	0.36	53.3	0.66	95.3

Linear fitting for kinetic parameters estimation was carried out involving only experimental points at lower temperatures (140, 160, 180 and 200 °C), as the conversion at 220 and 240 °C is higher and reaction rate could be affected by thermodynamic equilibrium. Table 3 summarizes the estimated kinetic parameters for the investigated samples. Activation energy is greater for second order kinetics; higher values for pre-exponential factor compensate this difference between the two models.
The resulting coefficient of determination (R^2) is quite high (above 0.98 for all the six fittings). Second order kinetic model leads to slightly better results in terms of least squares minimization.

Table 3: Kinetic parameters for methanol dehydration to DME assuming first and second order reaction

	1st order		2nd order	
Catalyst	$k_0\left(\frac{L}{g_{cat}\cdot s}\right)$	$E_a\left(\frac{kJ}{mol}\right)$	$k_0\left(\frac{L^2}{g_{cat}\cdot mol\cdot s}\right)$	$E_a\left(\frac{kJ}{mol}\right)$
ZSM-5_P	1.0 E+06	70.0	5.4 E+11	93.6
ZSM-5_30	2.8 E+06	74.1	5.9 E+11	94.5
ZSM-5_60	1.4 E+06	70.0	3.8 E+12	99.2

4. Conclusion

MFI-type zeolites were tested for methanol dehydration reaction to produce dimethyl ether (DME). *H form* zeolite (ZSM-5_P) performance was compared with its desilicated samples (ZSM-5_30 and ZSM-5_60). Characterization of acid sites via FT-IR spectroscopy analysis evidenced that desilicated sample ZSM-5_60 presents a greater amount of Bronsted acid sites than the other investigated zeolites (510 vs. ≈400 μmol per gram of catalyst). ZSM-5_60 sample showed superior catalytic activity especially at low/intermediate temperatures (up to 200 °C), confirming that methanol dehydration seems to preferentially occur over Bronsted acid sites. Conversion equal to 27 %, 26 % and 36 % was found at 160 °C for ZSM-5_P, ZSM-5_30 and ZSM-5_60, respectively. Turnover frequency (TOF) evaluation at 160 and 180 °C coherently led to very

similar values for the three samples, indicating that the amount of Bronsted acid sites plays a crucial role in determining the catalyst activity. Kinetic investigation was carried out by considering simple models; activation energy of about 70 and 95 kJ/mol was calculated for all the investigated catalysts by using 1st and 2nd order model, respectively.

References

Abate, S., Giorgianni, G., Lanzafame, P., Perathoner, S., Centi, G., 2016. Multifunctional HDO / Selective Cracking Ni / HBEA Catalysts to produce Jet Fuel and Diesel from Algal Oil, Chemical Engineering Transactions, 50, 3–4.

Aloise, A., Marino, A., Dalena, F., Giorgianni, G., Migliori, M., Frusteri, L., Cannilla, C., Bonura, G., Frusteri, F., Giordano, G., 2020, Desilicated ZSM-5 zeolite: Catalytic performances assessment in methanol to DME dehydration, Microporous and Mesoporous Materials, 302, 110198.

Areán, C. O., Platero, E. E., Mentruit, M. P., Delgado, M. R., i Xamena, F. L., García-Raso, A., Morterra, C., 2000. The combined use of acetonitrile and adamantane–carbonitrile as IR spectroscopic probes to discriminate between external and internal surfaces of medium pore zeolites. Microporous and mesoporous materials, 34(1), 55-60.

Brunetti, A., Migliori, M., Cozza, D., Catizzone, E., Giordano, G., Barbieri, G., 2020. Methanol Conversion to Dimethyl Ether in Catalytic Zeolite Membrane Reactors. ACS Sustainable Chemistry & Engineering, 8, 10471–10479.

Catizzone, E., Aloise, A., Migliori, M., Giordano, G., 2017, The effect of FER zeolite acid sites in methanol-to-dimethyl-ether catalytic dehydration, Journal of energy chemistry, 26(3), 406-415.

Catizzone, E., Giglio, E., Migliori, M., Cozzucoli, P., Giordano, G., 2020, The effect of Zeolite Features on the Dehydration Reaction of Methanol to Dimethyl Ether: Catalytic Behaviour and Kinetics, Materials, 2020, 13, 5577.

Catizzone, E., Aloise, A., Giglio, E., Ferrarelli, G., Bianco, M., Migliori, M., Giordano, G., 2021, MFI vs. FER zeolite during methanol dehydration to dimethyl ether: The crystal size plays a key role, Catalysis Communications, 149, 106214.

Dalena, F., Senatore, A., Iulianelli, A., Di Paola, L., Basile, M., Basile, A., 2019, Ethanol from biomass: future and perspectives, In Ethanol (pp. 25-59), Elsevier.

Daniell, W., Topsøe, N. Y., & Knözinger, H., 2001, An FTIR study of the surface acidity of USY zeolites: Comparison of CO, CD3CN, and C5H5N probe molecules, Langmuir, 17(20), 6233-6239.

Iulianelli, A., Jansen, J. C., Esposito, E., Longo, M., Dalena, F., Basile, A., 2019, Hydrogen permeation and separation characteristics of a thin Pd-Au/Al2O3 membrane: The effect of the intermediate layer absence, Catalysis Today, 330, 32-38.

Marchese, M., Giglio, E., Santarelli, M., Lanzini, A., 2020, Energy performance of Power-to-Liquid applications integrating biogas upgrading, reverse water gas shift, solid oxide electrolysis and Fischer-Tropsch technologies, Energy Conversion and Management: X, 6, 100041.

Meunier, F. C., Verboekend, D., Gilson, J. P., Groen, J. C., Pérez-Ramírez, J., 2012, Influence of crystal size and probe molecule on diffusion in hierarchical ZSM-5 zeolites prepared by desilication, Microporous and mesoporous materials, 148(1), 115-121.

Migliori, M., Aloise, A., Giordano, G., 2014, Methanol to dimethyl ether on H-MFI catalyst: The influence of the Si/Al ratio on kinetic parameters, Catalysis Today, 227, 138-143.

Migliori, M., Catizzone, E., Aloise, A., Bonura, G., Gómez-Hortigüela, L., Frusteri, L., Cannilla, C., Frusteri, F., Giordano, G., 2018, New insights about coke deposition in methanol-to-DME reaction over MOR-, MFI- and FER-type zeolites, Journal of Industrial and Engineering Chemistry, 68, 196-208.

Migliori, M., Condello, A., Dalena, F., Catizzone, E., Giordano, G., 2020, CuZnZr-Zeolite hybrid grains for DME synthesis: New evidence on the role of metal-acidic features on the methanol conversion step, Catalysts, 10(6), 671.

Papanikolaou, G., Lanzafame, P., Giorgianni, G., Abate, S., Perathoner, S., Centi, G. 2020, Highly selective bifunctional Ni zeo-type catalysts for hydroprocessing of methyl palmitate to green diesel, Catalysis Today, 345, 14–21.

Park, J., Cho, J., Park, M. J., Lee, W. B., 2020, Microkinetic modeling of DME synthesis from methanol over H-zeolite catalyst: Associative vs. dissociative pathways, Catalysis Today, In Press (DOI: 10.1016/j.cattod.2020.02.011).

Rownaghi, A. A., Rezaei, F., Stante, M., & Hedlund, J. 2012. Selective dehydration of methanol to dimethyl ether on ZSM-5 nanocrystals. Applied Catalysis B: Environmental, 119, 56-61.

Trombetta, M., Armaroli, T., Alejandre, A. G., Solis, J. R., Busca, G., 2000, An FT-IR study of the internal and external surfaces of HZSM5 zeolite, Applied Catalysis A: General, 192(1), 125-136.